

Model for growth of *a*-Si:H and its alloys

R. A. Street

Xerox Palo Alto Research Center, Palo Alto, California 94304

(Received 5 April 1991)

Alloys of *a*-Si:H with Ge, C, N, O, etc., have higher defect densities and poorer electronic properties than *a*-Si:H. Recent ideas of hydrogen equilibration during growth are used to explain the structural trends in the alloys responsible for the different electronic properties. The analysis finds two characteristically different types of behavior, distinguished by the hydrogen-bond strengths of the alloy elements. Type-1 alloys have predominantly silicon dangling bonds and a large disorder broadening of the valence-band tail, while type-2 alloys have dangling defects on the nonsilicon element and low disorder. Examples are *a*-Si:C:H and *a*-Si:Ge:H, respectively. The same approach to understanding the electronic structure is applied to alloys with halogens such as fluorine, to the different elemental hydrogenated amorphous semiconductors, and to microcrystalline thin films.

I. INTRODUCTION

Hydrogenated amorphous silicon (*a*-Si:H) is one of a broad class of plasma-deposited materials based on group-IV elements, in which the presence of hydrogen is crucial. *a*-Si:H is usually deposited from SiH₄ and contains about 10 at. % hydrogen, which terminates most of the silicon dangling bonds, giving a material with very low defect density. Many alloy materials are grown by the same technique; examples are *a*-Si:Ge:H, which is important in solar cell applications¹; *a*-Si:N:H, and *a*-Si:O:H, which are dielectrics used in thin-film transistors²; and *a*-Si:C:H, which acts as a transparent doped layer on solar cells and sensors³ and as an electroluminescence material.⁴ Polycrystalline silicon and diamond are grown in closely related plasma-deposited process using SiH₄ or CH₄, heavily diluted with hydrogen.^{5,6}

A perplexing aspect of the amorphous alloys is that all of them possess poorer electronic properties than *a*-Si:H. This discussion focuses on two of the most important parameters determining the electronic properties, namely, the dangling-bond defect density, and the inverse slope E_0 of the exponential valence-band tail density of states, which is reflected in the optical absorption edge. A broadband tail lowers the drift mobility, and a high defect density reduces the excited carrier lifetime, both of which are undesirable electronic properties. Some alloys, such as *a*-Si:Ge:H have a high defect density while retaining reasonably sharp band tails,⁷ while others, e.g., *a*-Si:C:H, have both a high defect density and broadband tails.⁸ In many cases, the poor electronic properties are related to structural features, such as a high density of voids or specific hydrogen bonding configurations,⁹ but without a clear explanation of why these features occur. This paper proposes a general explanation of the structure of this class of materials, which accounts for special nature of *a*-Si:H and the poorer properties of alloys. The model is also applied to the growth of polycrystalline silicon and diamond from a hydrogen-rich plasma.

II. GROWTH MODEL

The model of growth of amorphous alloys is based on the recent description of the interaction of hydrogen with the growing surface of the *a*-Si:H film, which makes the following assumptions.¹⁰

(1) During deposition from hydrogen-containing gases, the bonding structure of the film is in large part controlled by the effective hydrogen chemical potential in the plasma, μ_H . The hydrogen influences the structure through its reaction with the distribution of weak and broken silicon bonds.

(2) At sufficiently high growth temperature, μ_H in the plasma and the film tend to equalize because of the rapid interchange of hydrogen across the growth surface. The structure then approaches an equilibrium distribution of Si—Si and Si—H bonds, which minimizes the weak-bond and dangling-bond density, subject to the topological constraints of the amorphous network. The network constraint leads to minimum weak-bond disorder, as indicated by the valence-band tail slope which is not less than $E_0 \sim 40\text{--}50$ meV.

(3) At low growth temperature there is a kinetic constraint to the structural equilibration because insufficient hydrogen motion does not allow the network to rearrange between alternative configurations. Material grown in the kinetically limited regime has a higher disorder manifested by a broader distribution of weak bonds.

The model focuses on the effect of hydrogen chemical reactions on the growth structure. The detailed reactions of the impinging gas radicals (i.e., SiH₃, SiH₂, etc.) clearly also play a role in defining the structure.¹¹ The hypothesis of this paper is that the hydrogen reactions beneath the surface of the film change the structure from that which is created by the attachment of radicals at the surface to a structure which approaches a constrained equilibrium. In neglecting the specific surface chemical reactions, the model attempts to explain the general structural trends, but is not expected to account for all

the details.

The approach taken is to describe the hydrogen interactions in terms of a hydrogen density of states (HDOS) distribution, $N_H(E)$, which is illustrated in Fig. 1.¹² The energy is of the hydrogen bonding sites relative to the vacuum level, E_{HV} . Hydrogen resides in the occupied states below μ_H , which, in *a*-Si:H, are the Si—H bonds. No distinction is made here of the different hydrogen environments (i.e., the dilute and clustered hydrogen phases), except to represent these local variations by a broadened Si—H band.¹³ The band of unoccupied states above μ_H includes the distribution of weak Si—Si bonds into which hydrogen can insert with low energy, and stronger Si—Si bonds at high energy. The hydrogen migration energy, E_M , is indicated in Fig. 1, and corresponds to the average energy at which hydrogen can diffuse freely.

The energies of the different features of the HDOS are known only approximately, and are discussed further elsewhere.^{12,13} The migration energy E_M is estimated to be 0.5–1 eV below E_{HV} , based on information about the bond-center hydrogen site in crystalline silicon. The activation energy of 1.5 eV for hydrogen diffusion corresponds to the energy separation of E_M and μ_H (with a possible correction for the temperature dependence of μ_H). The peak of the Si-H band lies about 0.5 eV below μ_H , to account for the low equilibrium defect density in *a*-Si:H (see later discussion). These values place the Si—H bonds 2.5–3.0 eV below E_{HV} , which is roughly comparable with the expected Si—H bond strength.

The equilibration of the bonding structure induces a minimum in the hydrogen density of states at μ_H , because this configuration corresponds to the minimum defect density.¹⁰ This interaction between μ_H and the HDOS allows hydrogen to influence the distribution of weak Si—Si bonds and the density of dangling bonds, which together are two primary determinators of the electronic

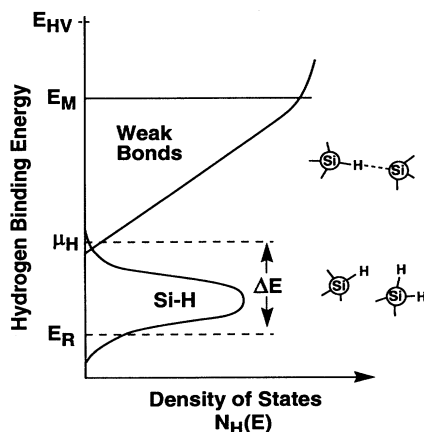


FIG. 1. Illustration of the hydrogen density of states for *a*-Si:H, showing the Si—H bonds and the energy of H in the distribution of Si—Si bonds. E_{HV} is the energy of hydrogen in vacuum, E_M is the effective migration energy of H in *a*-Si:H, μ_H is the hydrogen chemical potential, and E_R is the redistribution energy as defined in the text.

properties of the films. The distribution of weak bonds is characterized by the inverse slope, E_{WB} , of the assumed exponential distribution of hydrogen bonding sites; according to one of the weak bond models, $E_{WB} \sim 2E_0$.¹⁴

The model predicts the conditions for optimum growth of *a*-Si:H as follows. The surface layer formed by attaching highly hydrogenated gas radicals (e.g., SiH_3) has a high hydrogen concentration and is assumed to be highly disordered.¹⁰ The final film structure is determined in the subsurface region through the motion and elimination of the excess hydrogen, and the reduction in structural disorder. In order to obtain the optimum growth structure, it is assumed that a large fraction of the bonded hydrogen must redistribute within the time t_s in which the subsurface reactions establish the final film structure. The rate-limiting step in this process is attributed to the excitation of hydrogen to the mobile state at E_M , which occurs with rate $\omega_0 \exp[-(E_M - E)/kT]$, where E is the hydrogen energy. A redistribution energy E_R is therefore defined by equating the inverse of the excitation rate to the time t_s , giving

$$E_M - E_R = kT \ln(\omega_0 t_s), \quad (1)$$

where E_M is the hydrogen migration energy (see Fig. 1), and $\omega_s = 10^{13} \text{ sec}^{-1}$. E_R is indicated in Fig. 1 and separates those hydrogen atoms of higher energy which can move in time t_s from the deeper-lying states which cannot. It is difficult to give a precise value of t_s , but it is expected to be usually of order 10 sec, this being the typical time to grow a few atomic layers of the film.

It is a considerable simplification to assume that structural rearrangement takes place by excitation of hydrogen to E_M . In practice there is probably a range of excitation energies which depend on the details of the structural relaxation. For example, a close pair of Si—H bonds may interact directly to liberate H_2 without excitation over a large energy barrier. The excitation to E_M is the largest energy barrier to move hydrogen, and should therefore represent the rate-limiting step in the structural rearrangement. A limitation of the present model is that the complexities of the surface reactions are replaced by a single average process.

The assumption that most of the hydrogen must move in order to relax the network implies that the most ordered structure requires E_R to be sufficiently far down the Si-H band. If this condition is not met, then the structural ordering is kinetically limited and the material has a broader distribution of weak bonds. We do not know what fraction of the hydrogen needs to move to give the optimum structure, but guess that it is in the range 50–90%. An empirical expression for the valence-band tail slope (and weak-bond distribution) is

$$E_{WB}/2 = E_0 = E_0^{\min} + \beta_{\text{dis}}^E, \quad (2)$$

where β is the fraction of hydrogen which remains un-equilibrated. E_0^{\min} is the band tail slope of the ideal amorphous network. E_{dis} represents the additional disorder of a nonoptimal network and is estimated to be of order 100 meV, since the band tail slope in *a*-Si:H deposited at room temperature is about 150 meV,¹⁵ compared to the

most ordered structure for which $E_0^{\min} \simeq 50$ meV.

A low defect density in *a*-Si:H requires that μ_H is well above the Si-H band, otherwise a large fraction of these states are unoccupied and are dangling bonds. The position of the chemical potential of the hydrogen in the plasma is¹¹

$$E_{HV} - \mu_H = kT \ln(N_{H0}/N_{HP}), \quad (3)$$

where N_{HP} is the atomic hydrogen concentration of the plasma and N_{H0} is the inverse of the hydrogen quantum volume, $3 \times 10^{24} \text{ cm}^{-3}$.¹⁰ The dangling-bond density arising from Si—H bonds which lose hydrogen is related to μ_H in the film by

$$N_{DH} = \int N_H(E) [1 - f(\mu_H, E, T)] dE \\ \simeq N_{SiH}^{\text{total}} \exp \left[-\frac{\mu_H - E_H}{kT} \right], \quad (4)$$

where f is the Fermi function for the hydrogen occupation. The approximation on the right side of Eq. (4) assumes a δ -function SiH band and allows us to estimate that $\mu_H - E_H$ is about 0.6 eV for a defect density of 10^{15} cm^{-3} at 550 K, which is a typical value for *a*-Si:H. Defects are also formed when hydrogen occupies the weak-bond states, with density.

$$N_{DW} = \int N_W(E) f(\mu_H, E, T) dE, \quad (5)$$

where $N_W(E)$ is the weak-bond distribution. When the structure is equilibrated with a minimum defect density, $N_{DW} \sim N_{DH}$.¹⁴ For nonequilibrated structures, the two densities depend on the position of the chemical potential.

To satisfy simultaneously the conditions for low defect density and minimum disorder, good-quality material requires that μ_H is well above the Si-H band, while at the same time E_R must be as far as possible below the Si-H peak; otherwise the structure is kinetically limited and has increased disorder. (Note that a broad weak-bond distribution causes a high defect density through its overlap with μ_H , so that the kinetically limited structure has a high defect density regardless of the energy of μ_H). Combining Eqs. (1) and (3) gives

$$\mu_H - E_R = E_{HV} - E_M + kT \ln \left[\frac{\omega_0 t_s N_{HP}}{N_{H0}} \right]. \quad (6)$$

For typical plasma conditions we estimate $t_s = 10$ sec, $N_{HP} = 10^{13} \text{ cm}^{-3}$, and that $E_{HV} - E_M$ is about 1 eV, to obtain,

$$\mu_H - E_R = \Delta E \simeq 1 + 4kT \sim 1.2 \text{ eV at } 550 \text{ K}. \quad (7)$$

The estimate that μ_H is about 0.6 eV above E_H in *a*-Si:H indicates that E_R is approximately 0.6 eV below E_H . The two conditions for optimum growth are met, provided that the Si-H band is not too broad. The observation that the *a*-Si:H films are of good quality over a substantial range of deposition conditions indicates that ΔE is indeed large compared to the width of the Si-H band.

There is a substantial uncertainty in the numerical

value of ΔE which comes primarily from the lack of a precise value for E_M . The large uncertainties in the values of t_s and N_{HP} have less effect on ΔE because these parameters occur in the logarithmic term in Eq. (7).

Figure 2 describes the temperature dependence of μ_H and E_R , and illustrates the range of growth temperatures at which good-quality equilibrated films grow. The low-temperature limit occurs when E_R is at the energy of the Si-H band and corresponds to the onset of kinetically limited growth. This temperature is about 500 K for *a*-Si:H, which indicates that the Si-H band is roughly 1.5 eV from E_M . Note that the model associates the kinetic limit with the temperature at which hydrogen diffusion occurs, which is also at about 500 K in *a*-Si:H.¹⁶ The high-temperature limit to optimum film growth occurs when μ_H is too close to the Si-H band, resulting in a high defect density according to Eq. (4). The model suggests that the upper limit to the range of growth temperatures is increased by a high concentration of atomic hydrogen in the gas and is reduced if the hydrogen bonding band is particularly broad. This prediction is supported by recent experiments which have found that good-quality *a*-Si:H can be grown at high temperature in a remote hydrogen plasma-deposition system, which features a high H concentration.¹⁷

A. Type-1 alloys

The model attributes the poor electrical properties of alloys to the presence of different H bonding configurations. Figure 3 illustrates the HDOS of *a*-Si:C:H, and a similar model applies to alloys with nitrogen and oxygen, all of which are referred to as type-1 alloys. Table I shows that each of these elements forms a stronger bond with hydrogen than Si-H, and therefore the hydrogen-bonding states lie at lower energy by 0.8–1.5 eV.¹⁸ The difficulty in growing these alloys is immediately apparent; in order to prevent the formation of silicon dangling bonds, μ_H must be above the Si-H band, while the kinetic limitation is avoided only if E_R is below the C-H band. The large difference between the Si-H and C-H bonding energies prevents both conditions from being applied simultaneously.

The model predicts that the C—H (or N—H and O—H) bonds are not equilibrated in type-1 alloys grown

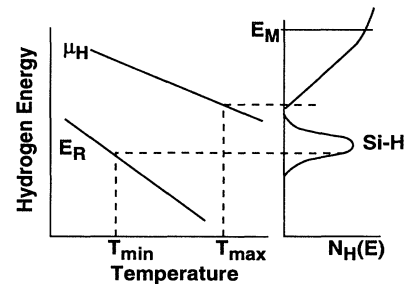


FIG. 2. Temperature dependence of the energies E_R and μ_H , showing the range of deposition temperatures which result in low density material.

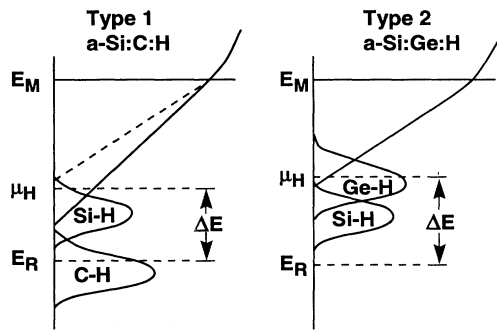


FIG. 3. Illustration of the hydrogen density of states for *a*-Si:C:H (type 1) and *a*-Si:Ge:H (type 2) alloys, showing the different hydrogen bonding states.

under the same conditions as for optimal *a*-Si:H. A broad distribution of weak bonds occurs because of the extra bonding disorder, and these tend to suppress μ_H and lead to high Si dangling-bond density. Carbon dangling bonds are not expected in the alloys because the C—H states lie well below μ_H . A continuous deterioration of the electronic properties is expected in the alloys because the fraction of nonequilibrated hydrogen increases with carbon concentration.

The experimental observations support the proposed model. The infrared spectra of *a*-Si:C:H alloys indicate a high density of CH₂ and CH₃ groups which are presumed to be formed during growth and remain because the hydrogen cannot equilibrate.⁸ The equivalent SiH₂ and SiH₃ groups are observed in *a*-Si:H films grown at low temperature¹⁹ and seem to be characteristic of kinetically limited growth structures. These bonding groups may reflect the deposition gas radicals which are unable to cross link because there is insufficient thermal energy to break the Si—H bonds. The valence-band tail of the type-1 alloys are broad, reflecting the additional disorder due a nonequilibrium structure, and the predominate defects are Si dangling bonds.⁸ The observed linear increase in the band tail slope with carbon concentration is consistent with Eq. (2). In addition, annealing studies find structural relaxation at elevated temperature, similar to that for *a*-Si:H grown at low temperature.²⁰

Of the three alloy elements, C, O, and N, the N—H bond is closest in energy to the Si—H bond (see Table I). The model therefore predicts that *a*-Si:N:H is the type-1 alloy which is easiest to deposit with good electronic

TABLE I. Bond strengths of various hydrogen bonds and SiF (Refs. 8 and 15).

Bond	Bond strength
Si—H	3.3 eV
C—H	4.3 eV
Ge—H	3.0 eV
N—H	4.1 eV
O—H	4.8 eV
Si—F	5.6 eV

properties. This material is indeed commonly used as a dielectric in thin-film transistors, in part because it has a relatively low defect density. On the other hand, it is well established that SiO₂ can be made as a much better dielectric with an extremely low defect density. However, the deposition conditions needed to obtain good-quality plasma-deposited SiO₂ (e.g. helium dilution)²¹ apparently do not involve significant hydrogen reactions. The present model only makes predictions about the properties of the films when growth is controlled by the hydrogen reactions, and does not preclude a better growth structure resulting from a different set of plasma reactions. The model also predicts how the structure of the type-1 alloys may be improved. The requirement to reduce E_R without changing μ_H may be achieved by raising the growth temperature and simultaneously diluting the plasma with hydrogen. This change in deposition conditions is found to improve *a*-Si:C:H alloys.²²

B. Type-2 alloys

a-Si:Ge:H is an example of the second type of alloy (type 2) in which the Ge—H bond is weaker than Si—H and therefore lies at higher energy in the density of states (see Fig. 3). In this case the same deposition conditions as for *a*-Si:H avoid the kinetic limitation, and a large broadening of the band tails is not expected. On the other hand, the Ge—H bonds are at sufficiently high energy that they intersect the chemical potential and therefore should result in many Ge dangling-bond defects, but few Si dangling bonds. Experiments again confirm these predictions. Alloying does increase the Ge dangling-bond density, often to above 10¹⁷ cm⁻³, while the Si dangling-bond density remains low,²³ and the alloys can be grown with a band tail slope no larger than 70 meV.⁷ Improved *a*-Si:Ge:H material should result from raising the H chemical potential above the Ge—H bands, for example, by hydrogen dilution of the plasma, and this process has indeed been shown to improve the Si-Ge alloys in some reports.²⁴ However, the assumption of a minimum disorder of the network implies that the weak-bond distribution overlaps the Ge—H bands and cause a high defect density irrespective of the energy of μ_H , as indicated in Fig. 3. It may not be possible to grow low defect density Ge-rich alloys. Growth of optimal Si-Ge alloys requires careful control of μ_H , and should be grown as close as possible to the conditions for the transition to microcrystallinity (see below).

Thus, both types of alloys tend to have higher defect densities than *a*-Si:H, but with characteristically different material properties. Type-1 materials have Si dangling bonds and broadband tails, while type-2 materials have dangling bonds of the other alloy element, and a narrow-band tail distribution.

C. Halogen substitutes for hydrogen

Another group of alloys to which the model can be applied are those containing halogen substitutes for hydrogen (e.g., *a*-Si:F:H). The replacement of hydrogen with fluorine is common, and in some cases is reported to im-

prove the material.²⁵ However, films with more F than H are of poor electronic quality.²⁶ Fluorinated *a*-Si:H has the properties of a type-1 alloy, since the Si-F band lies far below Si-H in a combined hydrogen and fluorine density of states. The redistribution energy E_R therefore lies above the Si-F band under typical growth conditions. Provided the fluorine content is sufficiently low (perhaps up to 20% of the hydrogen), the inability of the bonded fluorine to equilibrate may not degrade the structure significantly. However, the structure is kinetically limited at high F concentrations and therefore characterized by a high Si dangling-bond density and broadband tails. SiF₂ and SiF₃ bonding structures are expected to result from the kinetically limited Si—F bonds, and these have been observed in the films.²⁷

D. Elemental amorphous materials

The differences between the elemental hydrogenated amorphous semiconductors *a*-C:H, *a*-Si:H, and *a*-Ge:H can also be considered using the same approach. The HDOS of these materials are shown in Fig. 4. Assuming that these materials have similar minimum weak-bond distributions, then the model predicts that *a*-Ge:H intrinsically has the highest defect density of the three materials, because of the larger overlap between the weak bonds and Ge-H bands. The lowest defect densities reported for *a*-Ge:H are about $5 \times 10^{16} \text{ cm}^{-3}$, even with careful control of the hydrogen dilution of the plasma.²⁸ Although this reasoning suggests that *a*-C:H should have an even lower defect density than *a*-Si:H, the optimum growth temperature also increases across this composition sequence and is highest in *a*-C:H because of the strong C—H bonds. The increased growth temperature potentially increases the defect density because of the activated term in Eq. 4, but the actual defect density also depends on the position of the chemical potential and is difficult to predict because of the two offsetting effects. Experiments find that *a*-C:H can be made with as low a defect density as *a*-Si:H.²⁹ The model indicates that high-temperature growth with a high hydrogen dilution are the optimal deposition conditions. However, the model does not address the possibility of graphitic bonding in *a*-C:H films and its effect on the material properties.

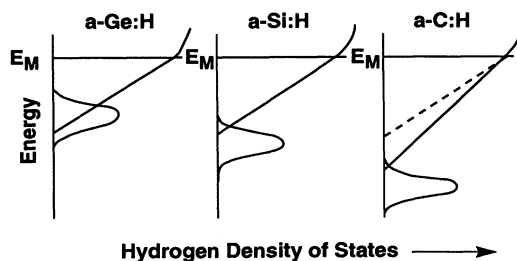


FIG. 4. Illustration of the hydrogen density of states for the elemental hydrogenated semiconductors, *a*-Ge:H, *a*-Si:H, and *a*-C:H.

E. Plasma-deposited crystalline films

The final application of the model to be considered is the growth of polycrystalline films from a hydrogen plasma. The transition from amorphous to crystalline growth induced by the high dilution of silane by hydrogen in the plasma is attributed in the model to a chemical potential which is high up in the weak bond band.¹⁰ The crystalline structure occurs because the weak-bond distribution of the amorphous phase is unstable to hydrogen reactions. Crystalline films are expected to occur most readily at the lowest temperature at which the kinetic limit is avoided, because further increase of temperature reduces the hydrogen chemical potential, according to Eq. (3). We therefore expect that the optimum growth temperatures of both amorphous and crystalline phases are similar. The same arguments should apply to silicon films and to diamond, which is also deposited from a hydrogen-rich plasma. Diamond thin films are typically grown at 600°C or above, compared to about 250°C for microcrystalline silicon.⁶ The higher temperature is consistent with the stronger C—H bond compared to Si—H and suggests that a similarly high temperature should be used to grow optimal *a*-C:H and possibly also *a*-Si:C:H alloys.

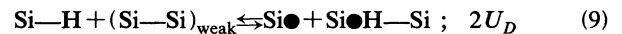
III. RELATION TO THE WEAK-BOND MODEL

The model presented in this paper associates the equilibrium defect densities with the position of the hydrogen chemical potential in the H density of states [Eqs. (4) and (5)]. Previously the defect density has been successfully explained by the weak-bond model,^{30,31} which describes the defect-formation energy U_D in terms of electronic states in the band gap,

$$U_D = E_D - E_{VB} , \quad (8)$$

where E_D is the gap state energy of the defect and E_{VB} is valence-band tail energy associated with the weak bond. At first sight there seems to be no connection between these models, since one relates the defect-formation energy only to the gap states without involving hydrogen, while the other relates the defects to hydrogen bonding energies without considering the electronic states.

The two models are, however, closely related. Consider, for example, the chemical reaction



where Si● represents a dangling-bond defect and $2U_D$ is the energy of the reaction. The reaction corresponds to the excitation of hydrogen from the Si-H band into the weak-bond states in the HDOS of Fig. 1. The reaction equally corresponds to the conversion of a weak bond into two dangling bonds. Street and Winer showed that the assumption of the weak-bond model that only electronic energies contribute to the defect-creation energy [Eq. (8)] allows a mapping of the electronic density of state onto the HDOS.¹⁴

Figure 5 compares the two density of states distributions and illustrates the relation between the energies as reaction (9) proceeds. The HDOS is taken from Fig. 1

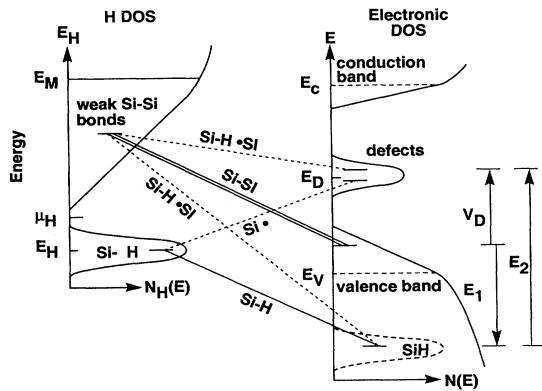


FIG. 5. Illustration of the mapping between the HDOS (left) and the electronic DOS (right) based on the assumptions of the weak-bond model. The lines show the relation between the states for the defect-creation mechanism defined by reaction (9). Solid lines are the left side of reaction (9) $[\text{Si-H} + (\text{Si-Si})_{\text{weak}}]$, and dashed lines are the right side $(\text{Si}\bullet + \text{Si-H}\bullet\text{Si})$.

and the electronic DOS is the usual description of *a*-Si:H, with localized band tails and a defect state in the gap. The Si—H bond has electronic states deep in the valence band, while the Si-Si weak bonds are associated with valence-band tail states. The bond contains two electrons and corresponds to two levels in the one-particle electronic DOS. The release of hydrogen from Si-H converts this state into a dangling-bond defect with electronic states in the gap. The insertion of the hydrogen into the weak bond splits the two energy levels; one becomes a dangling-bond defect and the other an Si—H bond. (It is assumed that the H bonding is very asymmetrical in a sufficiently weak bond.) The different energy-level splittings for the states is indicated in Fig. 5, from which the total energy of the reaction is $U_D + E_2 - E_1$ which equals $2U_D$, provided that the Si—H bonds on the two sides of the reaction have similar energies.

The mapping of the hydrogen and electronic DOS distributions follows from Eq. (8) and depends on it being correct. The expression for the defect-formation energy neglects the contributions to U_D from the changes in the other bonding electrons and from the ion-core interactions. In particular, the model depends on the assumption that the Si—H bonds in the two configurations are similar. It is not obvious that this should be the case, although the bonds may not be significantly perturbed by their surroundings if the Si—Si bond is sufficiently weak. Although the weak-bond model gives a good quantitative description of the defect density, the assumptions have not yet been verified by theory.

The HDOS model describes the formation of two defects, while only one defect is involved in Eq. (8). Thus, the slope of the assumed exponential distribution of weak bonds is twice that of the valence-band tail, as was noted in Sec. II. Reaction (9) is not the only possible model for hydrogen-induced defect creation.¹⁴ Other mechanisms in which hydrogen reacts with weak bond to form defects

also allow a mapping between the two density-of-states distributions.

The situation in the alloys is further complicated. The weak bond model predicts that the defect densities are different in the alloys, because of the change in band gap energy and of the gap state energy levels of different types of defects. For example, in *a*-Si:Ge:H alloys, the Si and Ge dangling bonds have formation energies

$$U_D(\text{Si}) = E_{\text{VB}} - E_D(\text{Si}\bullet), \quad U_D(\text{Ge}) + E_{\text{VB}} = E_D(\text{Ge}\bullet).$$

$E_{\text{VB}} - E_D(\text{Si}\bullet)$ presumably decreases upon alloying with germanium, because of the shrinking of the band-gap energy, which moves the band edge closer to the defect state, and suggests that the Si dangling-bond density should increase. The model predicts that Ge dangling-bond density is larger than the Si density provided that the $\text{Ge}\bullet$ defect level is closer to the valence band than $\text{Si}\bullet$.

The shrinking of the gap with alloying is not included in the HDOS description of the defect creation. Instead the difference between the Ge and Si defect density are related to the different binding energies of Ge-H and Si-H, rather than to the different gap state energies. Further, neither model makes a distinction between the different possible types of weak-bond states (i.e., Si-Si, Ge-Ge, and Si-Ge). These may have different energies in the HDOS and also different energies in the valence-band tail states, which would affect both the calculations of the defect densities. The simple model which allows a mapping of the gap state energies onto the HDOS does not seem to apply to the alloys. A much more detailed knowledge of the bond energies and their associated gap states is needed to clarify the relation between the two models.

IV. CONCLUSIONS

The model described here attributes the lower electronic quality of *a*-Si:H-based alloys to the presence of different hydrogen binding energies to the alloy elements. This makes it difficult to achieve the necessary conditions of almost full occupancy of the H bonding sites and sufficient mobility of the hydrogen to equilibrate the structure. Type-1 alloys are those with elements having a stronger hydrogen bond than Si-H. The kinetic limit imposed by the slower migration of hydrogen causes a disorder broadening of the weak bonds and extra silicon dangling bonds. Type-2 alloys have weaker hydrogen bonds, and are less susceptible to a kinetic limitation to the structure. However, the H bonding band tends to overlap with the weak-bond distribution, resulting in a large dangling-bond density, but of the alloy element rather than silicon.

ACKNOWLEDGMENTS

Many helpful discussions with W. Jackson are gratefully acknowledged. The research was supported by the Solar Energy Research Institute.

- ¹See, for example, S. Wagner, V. Chu, J. P. Conde, and J. Z. Liu, *J. Non-Cryst. Solids* **114**, 453 (1989), and references therein.
- ²K. D. Mackenzie, A. J. Snell, I. French, P. G. LeComber, and W. E. Spear, *Appl. Phys.* **31**, 87 (1983).
- ³Y. Tawada, H. Okamoto, and Y. Hamakawa, *Appl. Phys. Lett.* **39**, 237 (1981).
- ⁴D. Kruangam, M. Deguchi, Y. Hattori, T. Toyama, H. Okamoto, and Y. Hamakawa, in *Amorphous Silicon Semiconductors—Pure and Hydrogenated*, edited by A. Madan, M. Thompson, D. Adler, and Y. Hamakawa, MRS Symposia Proceedings No. 95 (Materials Research Society, Pittsburgh, 1987), p. 609.
- ⁵A. Matsuda, *J. Non-Cryst. Solids* **59&60**, 767 (1983).
- ⁶For a series of papers, see *J. Mater. Res.* **5**, 2273 (1990).
- ⁷H. C. Weller, S. M. Paasche, C. E. Nebel, F. Kessler, and G. H. Bauer, in *Proceedings of the 19th IEEE Photovoltaic Specialists Conference, New Orleans* (IEEE, New York, 1987), p.872; S. Guha, J. S. Payson, S. C. Agarwal, and S. R. Ovshinsky, *J. Non-Cryst. Solids* **97&98**, 1455 (1987).
- ⁸For a review and references see J. Bullot and M. P. Schmidt, *Phys. Status Solidi B* **143**, 345 (1987).
- ⁹A. H. Mahan, D. L. Williamson, and B. P. Nelson, in *Amorphous Silicon Technology-1989*, edited by A. Madan, M. J. Thompson, P. C. Taylor, Y. Hamakawa, and P. G. LeComber, MRS Symposia Proceedings No. 149 (Materials Research Society, Pittsburgh, 1989), p.539.
- ¹⁰R. A. Street, *Phys. Rev. B* **43**, 2454 (1991).
- ¹¹A. Gallagher and J. Scott, *Solar Cells* **21**, 147 (1987).
- ¹²R. A. Street, *Solar Cells* **30**, 207 (1991).
- ¹³For recent work which discusses the energies of different possible H configurations, see W. B. Jackson, *Phys. Rev. B* **41**, 10257 (1990).
- ¹⁴R. A. Street and K. Winer, *Phys. Rev. B* **40**, 6236 (1989).
- ¹⁵See M. Stutzmann, *Philos. Mag. B* **60**, 531 (1989).
- ¹⁶D. E. Carlson and C. W. Magee, *Appl. Phys. Lett.* **33**, 81 (1978).
- ¹⁷N. M. Johnson, C. E. Nebel, P. V. Santos, W. B. Jackson, R. A. Street, K. S. Stevens, and J. Walker, *Appl. Phys. Lett.* **59**, 1443 (1991).
- ¹⁸P. W. Adkins, *Physical Chemistry* (Freeman, San Francisco 1978), p. 111.
- ¹⁹G. Lucovsky, R. J. Nemanich, and J. C. Knights, *Phys. Rev. B* **19**, 2064 (1979).
- ²⁰K. Winer, *Appl. Phys. Lett.* **55**, 1759 (1989).
- ²¹J. Batey, E. Tierney, J. Stasiak, and T. N. Nguyen, *Appl. Surf. Sci.* **39**, 1 (1989); Z. Yin, D. V. Tsu, G. Lucovsky, and F. W. Smith, *J. Non-Cryst. Solids* **114**, 459 (1989).
- ²²S. H. Baker, W. E. Spear, and R. A. G. Gibson, *Philos. Mag. B* **62**, 213 (1990).
- ²³M. Stutzmann, R. A. Street, C. C. Tsai, J. B. Boyce, and S. E. Ready, *J. Appl. Phys.* **66**, 569 (1989).
- ²⁴K. Tanaka and A. Matsuda, *Mater. Sci. Rep.* **2**, 139 (1987).
- ²⁵A. Madan and S. Ovshinsky, *J. Non-Cryst Solids* **35&36**, 171 (1980).
- ²⁶M. Janai and R. A. Street, *Phys. Rev. B* **31**, 6609 (1985).
- ²⁷L. Ley, K. J. Grunz, and R. L. Johnson, in *Proceedings of the Conference on Tetrahedrally Bonded Amorphous Semiconductors*, edited by R. A. Street, D. K. Biegelson, and J. C. Knights, AIP Conf. Proc. No. **73** (AIP, New York, 1981), p. 161.
- ²⁸W. Paul, S. J. Jones, F. C. Marques, D. Pang, W. A. Turner, A. E. Wetsel, P. Wickboldt, and J. H. Chen, in *Amorphous Silicon Technology-1991*, edited by A. Madan, Y. Hamakawa, M. J. Thompson, P. C. Taylor, and P. G. LeComber, MRS Symposia Proceedings No. 219 (Materials Research Society, Pittsburgh, 1991), p. 211.
- ²⁹A. Reyes-Mena, R. Asomota, J. Gonzalez-Hernandez, and S. S. Chao, *J. Non-Cryst. Solids* **114**, 310 (1989).
- ³⁰Z. E. Smith and S. Wagner, *Phys. Rev. Lett.* **59**, 688 (1987).
- ³¹M. Stutzmann, *Philos. Mag. B* **56**, 63 (1987).